

## ***Interactive comment on “Impact of a new emission inventory on CAM5 simulations of aerosols and aerosol radiative effects in eastern China” by Tianyi Fan et al.***

**Tianyi Fan et al.**

fantianyi@bnu.edu.cn

Received and published: 26 February 2017

We thank the referees' valuable comments and suggestions on the improving the scientific significance of this work. Here, we attempt to further explore this research topic by discussing the impact of emission uncertainty on aerosol and aerosol radiative effect (ADRE) over eastern China in the last decade, missing sources of aerosol mass in the winter, and the observed seasonality of sulfate aerosol concentration. Here are some discussions: Responds to Referee #1's comments: Referee: "China SO<sub>2</sub> emission has been declined since 2006 while NO<sub>x</sub> and NH<sub>3</sub> have been increasing. What's the change in aerosol radiative forcing over China in the decade as the change in emission structure? Is it significantly different from the simulation uncertainty as using the

C1

different emissions of MEIC and IPCC AR5?" The referee addressed a very important question. We estimate the historical and future change of ADRE based on climate models. However, the uncertainty of aerosol emissions used in the climate models could add another dimension of uncertainty in simulating the change of aerosol concentration and the radiative effect. As mentioned by the referee, the emission structure changed in China during the last decade (2006-2015). The emission of SO<sub>2</sub> decreased by 9.2% from 34.0 Tg in 2006 to 30.8 Tg in 2010 (-2.4% annual growth rate) (Lu et al., 2011). The NH<sub>3</sub> emission decreased from 10.5 Tg in 2006 to 9.7 Tg in 2012 with an annual rate of 1.4% (Kang et al., 2016). Meanwhile, some researches show that the emissions of BC, OC, and NO<sub>x</sub> have been increasing since 2006. The BC/OC emissions increase from 1.6 Tg/3.6Tg in 2004 to 1.9 Tg/4.0 Tg in 2010, with an annual growth rate of 2.8%/1.7%. The MEIC developer team estimates that the emission of BC/OC decreased from 2006 to 2010 due to reduced emissions in the domestic and transportation sectors. The NO<sub>x</sub> emission grew by 113.9% from 12.2 Tg in 2000 to 26.1 Tg in 2010, with an annual growth rate of 7.9% from 2000-2010 (Zhao et al., 2010). To examine the change in the ADRE as the change in the emission structure, we carry out simulation using MEIC emission from 2002 to 2012. We choose these 11 years because China's economy recovered from a depression in 2002, and since then the SO<sub>2</sub> emission start to grow dramatically and decrease after 2006 due to the application of desulfurization equipment. After 2012 the annual emission rates do not change as dramatically as the previous years. To avoid the impact of decadal trend of meteorological variations, we use the reanalysis wind in 2009 to nudge the model winds towards the "constrained meteorology" for all the years from 2002 to 2012. In this way, the change of aerosol concentrations are mostly controlled by the change of emission alone since the meteorological factors (wind speed, temperature, and etc.) are identical among the years.

Figure 1C shows the MEIC aerosol and gas precursor emission trend from 2002 to 2012 in eastern China. Since gridded MEIC emission data are only available for 2008, 2010, and 2012, we scale the spatial distribution and seasonal variation of other years

C2

during the period to the 2008 gridded emission with the annual emissions. The annual emission rates of each species (SO<sub>2</sub>, BC, OC) are estimated by the MEIC developer team. The annual trends are consistent with other researches (Lu et al., 2011; Lei et al., 2009) although the absolute values are different. We keep using the MEIC estimations because their fuel usage is based on China Energy Statistical Yearbook (CESY) as the dataset based on the same algorithm as the gridded MEIC emission data that we used for 2009. Each species in each sector (power, energy, residential, and transportation) has a different scaling factor. The AR5 emissions from 2002 to 2009 are linearly interpolated from the only two estimates provided in the decade, that is, year 2000 and 2010. Emissions in 2011 and 2012 are set to be equal to year 2010. The uncertainty range of the MEIC SO<sub>2</sub> emission is also shown in Figure 1C. The overall uncertainties of MEIC emissions for China in 2006 are estimated to be  $\pm 12\%$  for SO<sub>2</sub>,  $\pm 31\%$  for NO<sub>x</sub>,  $\pm 68\%$  for NMVOC,  $\pm 208\%$  for BC, and  $\pm 258\%$  for OC (Zhang et al., 2009). The uncertainty range is a measure of how confidence we are about the estimated emission inventory. The uncertainties for each species are calculated by the combined uncertainties of the emission measurement and the activity levels. It is measured as 95% of confidence intervals (calculated as 1.96 times coefficient of variation, which is the standard deviation divided by the mean)(Streets et al., 2003), meaning that in 95% of circumstances the SO<sub>2</sub> emission, for example, is within  $\pm 12\%$  of the estimated value. The AR5 emissions of BC, OC, and SOAG are within the large uncertainty range of MEIC. However, the AR5 emission of SO<sub>2</sub> is outside the uncertainty range of MEIC except for year 2010 to 2012. We do not scale the SOAG species since the anthropogenic VOC species have large uncertainty and are not the dominant contributor as the natural biogenic VOCs are. Unfortunately, the chemistry and aerosol microphysical processes of nitrate aerosol are not incorporated in this research. According to our latest estimation the nitrate aerosol using MEIC emission inventory improves over 60% of the underestimated AOD compared with MODIS AOD retrieval in eastern China. Figure 2C shows that the change of the ADREs from 2002 to 2012 relative to those in 2002 are 0.02~0.24 W/m<sup>2</sup>, -0.38~0.1 W/m<sup>2</sup>, and -0.07~0.57 W/m<sup>2</sup> at TOA, surface

C3

and in the atmosphere, respectively. The decadal trend of ADRE agrees with the trend of emissions as shown in Figure 1C. Compare with the difference between the ADREs simulated by MEIC and AR5 emission inventories in 2009, which is -0.19 W/m<sup>2</sup>, -2.42 W/m<sup>2</sup>, 2.23 W/m<sup>2</sup> at TOA, surface and in the atmosphere, respectively, the decadal change is comparable to the uncertainty range introduced by the emission inventories. So as to answer the question by the referee, the change of ADRE in eastern China due to the change of emission structure is not significantly different than the difference estimation of the emission. It highlights the uncertainty of the emission inventories and the need of constraining the emission inventories of aerosol and precursors by in-situ and satellite observations. Our simulated decadal trend of ADRE agrees with previous findings. While decadal long observations of aerosol radiative trend over China are hard to obtain, decadal trend is often studied based on model studies. Li et al. (2014) shows that the clear-sky anthropogenic ADRE at surface increase since 2000 and peaks in the late 2000s for about -6 ~ -7 W m<sup>-2</sup>. Westervelt et al., (2015) shows that the aerosol radiative forcing decreases by about -0.8 W m<sup>-2</sup> in east Asia during 2005-2015 based on GFDL-CM3 model using RCP2.6 emission scenario, which shows decreasing trend of SO<sub>2</sub> emission after 2005. Bhawar et al., (2016) shows that over East Asia smoke region the linear trend of ADRE is -0.43 W/m<sup>2</sup>/year during 2001-2012 based on CSIRO MK-3.6.0 model results.

Referee: "Secondly, there are large model biases in winter which cannot be explained by emissions alone and the author has no discussion. . . . The model bias should be further discussed, and the implications to the conclusion should be mentioned. Thirdly, the observations in Figure 9 are susceptible. The observations show minimum winter sulfate in northern China cities, which is totally opposite to the general recognition that aerosols are higher in winter than in summer. An explanation is required." The second and the third comments are about the seasonal variation of simulated aerosol concentrations, so we respond to the two commons together. As shown in Figure 3C, the emission of SO<sub>2</sub> peaks in the winter in northern China (Harbin, Chengde, Shangdianzi, Beijing, Tianjin, Shijiazhuang, and Zhengzhou) due to heating in the domestic section.

C4

However, the model simulates the sulfate aerosol concentrations having their minimum in the winter (Figure 9), which is commonly seen for many climate models (personal communication with Prof. Liao Hong from Nanjing University of Information Science & Technology). Obviously, as mentioned by the referee, the surface concentration cannot be explained by emissions alone. We examine the processes that determine the sulfate aerosol concentration in the model, including gas-phase and aqueous-phase production rates, the dry and wet removal rate, and the controlling meteorological variables (Figure 3C). Figure 3C shows that the simulated seasonal variation of surface concentrations of sulfate aerosol are controlled by the gas-phase and aqueous-phase production processes, as oppose to the emission rate of SO<sub>2</sub>. CAM5-MAM3 included simple gas-phase photochemical oxidation by OH and aqueous-phase oxidation in cloud water by H<sub>2</sub>O<sub>2</sub> and O<sub>3</sub> (Lamarque et al., 2010; Tie et al., 2001). The aerosols formed in cloud have a chance to be “resuspended” to add interstitial aerosols. Gas-phase chemistry is most active in the summer due to the temperature-dependence of the reaction rate in the photochemical oxidation of SO<sub>2</sub> by OH. The aqueous-phase formation of sulfate aerosol also peaks in the summer due to high relative humidity. Both of gas-phase and aqueous-phase oxidations are inefficient in the winter although MEIC emission is much higher in the winter. The seasonal variation of modeled sulfate aerosol concentration is verified by some observations (Zhao et al., 2013; Zhang et al., 2013; Geng et al., 2013). However, observations from CAWNET (Zhang et al., 2012) show that sulfate aerosol in northern Chinese cities peaks in the winter as opposed to summer in spite of a minor maximum in the summer, which is consistent with our general recognition (Figure 4C). The contrasting result in observations could be due to different location and time. The difference between the simulated and the observed seasonal variation by the CAWNET may reveal that some mechanisms of sulfate aerosol formation in the winter over China are missing in the model. As indicated by the referee, “the importance of sulfate production through heterogeneous reactions of SO<sub>2</sub> on deliquescence preexisting particles catalyzed by transition metal ions, which can increase PM<sub>2.5</sub> concentrations and the mass fractions of secondary inorganic aerosols in the winter-

C5

time hazes of northern China (Wang et al. 2014; Huang et al., 2014; Zheng et al, 2015; Chen et al., 2016; Dong et al., 2016). The coexistence of NO<sub>2</sub> and SO<sub>2</sub> also promotes sulfate production (He et al., 2014; Wang et al., 2014)”. The aqueous-phase oxidation of SO<sub>2</sub> by NO<sub>2</sub> (Wang et al., 2016) or O<sub>3</sub> (Palout et al., 2016) is efficient to form sulfate aerosol under high relative humidity and NH<sub>3</sub> neutralization conditions. It is also possible that the wet scavenging is underestimated in the summer so that the ADRE maximum in the summer is overestimated.

Specific comments Line 113-115, What are the emission amounts in sectors of shipping, agricultural waste burning, waste treatment and natural biomass burnings? Are they high comparing to MEIC emissions? The emission amounts in sectors of shipping, agricultural waste burning, waste treatment and natural biomass burning are not included in MEIC emission. Therefore we keep them the same as the AR5 emission.

Line 130-140, I don't fully understand this paragraph. Did the model use BVOC from MEGAN model in MOZART-4 and use anthropogenic VOC from MEIC? Yes, the referee's understanding is basically correct. We rewrite the description in line as follows: “Since the IPCC AR5 dataset does not provide emissions of biogenic VOCs, the SOAG emission is derived from the emission fluxes of five primary VOC categories (isoprene, monoterpenes, big alkanes, big alkenes, toluene) that are prescribed from the Model for Ozone And Related chemical Tracers version 4 (MOZART-4) dataset (Emmons et al., 2010), in which the biogenic emissions of isoprene and monoterpenes are based on the Model for Emissions of Gases and Aerosols Emissions from Nature (MEGAN) (Guenther et al., 2006). The MEIC emission provides anthropogenic sources of the five VOC categories and the mapping table for lumping the MEIC VOC species to MOZART refers to Li et al. (2014). Since the MEIC does not provide the biogenic sources of isoprene and monoterpenes, which are much larger than their natural counterparts, we make their total emissions from anthropogenic and natural sources the same as those in the AR5 emission.

Line 140-142, Did the factor of 1.4 also apply to the natural biomass burning emissions

C6

to derive SOAG? Yes, it does. When deriving SOAG emission, all anthropogenic and biomass burning sectors are added up and multiplied by 1.4 to convert OC (carbon mass) to POM (organic mass).

Line 147, Is there particle number emissions in the AR5 emission inventories? No, the particle number emission in the AR5 emission inventory is not provided. The number concentration in both AR5 and MEIC emissions are calculated from the mass concentration as described in the text. To be more clear, the paragraph is rewritten as follows: "The number emission fluxes in both AR5 and MEIC are calculated from the mass fluxes in a consistent way. The mass to number conversion is based on  $E_{\text{number}} = E_{\text{mass}} / ((\pi/6) \bar{D}_v^3 \rho)$ , where  $\bar{D}_v$  is the volume-mean emitted diameter and  $\rho$  is the aerosol particle density (Liu et al., 2012). Since the MEIC emission does not provide mass emissions from agricultural waste burning, waste treatment, forest fire, grass fire and continuous volcanoes, we use the number fluxes from the AR5 emission for these sectors."

Line 170, The simulated ADRE is a "all-sky" value while the observation-deriving ADRE in Line 187 is "clear-sky". Need to state the discrepancy. The cloud-screening method (clear-sky) in observations neglects the effect of aerosol above and below clouds. Absorption of reflected solar radiation by absorbing aerosol above clouds should result in larger radiative warming effect. The radiative cooling by scattering aerosol below clouds is not as strong as in clear sky due to less sunlight penetrating the clouds. Both of the two factors will result in lower (more negative at TOA) radiative effect in clear-sky than that in all-sky. Therefore, the observation-derived ADRE in clear-sky provides an upper-limit of the model-estimated all-sky ADRE at TOA.

Line 211, It might be more appropriate to show concentration results (Section 3.2) before AOD results (Section 3.3). Thank you for the suggestion. It is more conventional to show surface concentration before AOD. Nevertheless, we show AOD first since we would like to address the question of whether the underestimated AOD by models is improved by using MEIC emission. Also, since satellite retrieved AOD provides the

C7

spatial distribution to be compared with the model results, we think it might be acceptable to show AOD before concentration results.

Line 240, why not show the results by aerosol components? The AOD by aerosol components has been added in the appendix.

Line 249, "while the observed maximum extends further north" According to Figure 5, it seems that the observed AOD maximum is in the south of the simulated maximum. Please rewrite this sentence. Line 250-251 have the same problem. We delete rewrite the sentences as "The model simulates a maximum between 35oN and 40oN in early summer (from May to July) which is to the north of the observed AOD maximum."

Line 249, "This model maximum is mostly due to dust aerosol . . ." It seems that the maximum AOD in the earlier summer is about half less than the observation, and the maximum AOD is from dust. Thus, the anthropogenic AOD is quite low comparing with MODIS. That is, CAM5 model heavily underestimates AOD in China and this cannot be explained by emissions alone. Besides to the emissions, the author need to mention other causes (e.g. missing nitrate, particle size distribution, aerosol hygroscopic growth, etc.) that account for the large AOD bias. We agree with the referee that other causes beside emission also account for the large AOD bias. We mentioned the plausible causes and future effort to be made in Line 258-262 and the summary section (Line 443-449). We rewrite the sentences as "This model maximum is mostly due to dust aerosol transported from the west, while the satellite retrievals do not show such strong dust emission and transport. The timing and location of dust aerosol in the model is biased. Since the dust emissions are the same in the simulations using the MEIC and AR5 emissions, the difference of the modeled AOD maximums between 35oN and 40oN is mainly due to sulfate condensed on dust aerosol. We notice that the maximum AOD in the satellite retrieval occurs around 30oN in early summer (May to July), as oppose to 35oN to 40oN as simulated by the model. The observed AOD maximum complies with the SO2 emission maximum in early summer around 30oN. Therefore, it is likely that this AOD maximum is due to sulfate aerosol formation and

C8

it is heavily underestimated by the model. Since the uncertainty of SO<sub>2</sub> emission is relative low ( $\pm 12\%$ ), this underestimation cannot be explained by emission alone. ”

Line 329-330, “The sulfate concentrations in northern China are characterized by the summer maximums” In Figure 9, at northern cities, the minimum wintertime sulfate in observations are susceptible. As the observations were collected from literature measurements that were carried out in different periods, the observations in summer and winter may not be comparable. The comparison uncertainty should be admitted. The summer maximums of the surface concentration of sulfate at northern cities in 2009 and 2010 are observed by some independent researches (Zhao et al., 2013; Zhang et al., 2013; Geng et al., 2015). It is possible that SO<sub>2</sub> to sulfate conversion is efficient in the summer due to high temperature and relative humidity. There are also observations showing opposite seasonal variations with sulfate concentration peaking in the winter during other periods (Zhang et al., 2012). The contrasting result in the observations could be due to different location and time.

Line 343-349, in my opinion, gas-phase oxidation of SO<sub>2</sub> is not the main pathway for sulfate production. Aqueous oxidation in droplet/cloud water should be more important. At 35o-40oN, the maximum sulfate difference between MEIC and AR5 in summer is also due to the high ambient humidity. Besides, if CAM5 can capture the wintertime high concentrations, the largest sulfate burden difference could be in winter than in summer. We totally agree with the referee. We add the seasonal variation of relative humidity in Figure 11. One thing to notice is that aqueous-phase oxidation occurs only in cloud droplets in the model. The aqueous-phase oxidation of SO<sub>2</sub> by NO<sub>2</sub> on pre-existing aerosols is not modeled by CAM5-MAM3, which is important in China (Wang et al., 2016). The model results show that the aqueous-phase oxidation is as important as the gas-phase chemistry. If we consider the oxidation by NO<sub>2</sub> on pre-existing aerosols, the contribution of aqueous-phase chemistry could be more important. Technical notes If possible, mark the data range (i.e. Min, Max) in Figure 7 and 9. Data range (one standard deviation) in Figure 7 and Figure 9 are marked. The standard deviations of

C9

the surface concentrations are provided in only three locations (Beijing, Zhengzhou, and Guangzhou) by the literatures. We add them to Figure 9. Figure 9. Error bars stand for one standard deviations of the observations. Figure captions:

Figure 1C. The change of emission rates of SO<sub>2</sub>, BC, OC, and SOAGs from year 2002 to 2012 in eastern China. The shaded areas are the uncertainty ranges of MEIC SO<sub>2</sub> emission. The uncertainty ranges of POM, BC, and SOAG ( $\pm 256\%$ ,  $\pm 208\%$ , and  $\pm 68\%$ , respectively) fulfill the plot range.

Figure 2C. The change of ADREs at TOA, surface and in the atmosphere relative to year 2002 with MEIC emission in eastern China.

Figure 3C (From left to right columns): (1) SO<sub>2</sub> emission rates from MEIC (black) and AR5 (blue) inventories, (2) gas-phase chemistry production in the simulations by MEIC (black) and AR5 (blue) and the surface temperature (red), (3) aqueous-phase production rates (black and blue) and the relative humidity at surface (red), (4) dry deposition rate (black and blue) and the 10-meter wind speed (red), and (5) wet scavenging rate (black and blue) and the precipitation rate (red).

Figure 4C. Seasonal variations of surface sulfate concentration at three locations (Gucheng, Panyu, and Zhengzhou) from CAWNET from 2006 to 2007. For comparison, the observations near the three locations used in our study (Beijing, Guangzhou, Zhengzhou) from 2009 to 2010 are also shown in dots.

Figure S1. The seasonal variation of longitudinal averaged (100oE-124oE) AOD at 550 nm by aerosol components (dust, sulphate, BC, POM, and SOA from top to bottom) simulated by CAM5-MAM3 using the MEIC emission (left column) and the AR5 emission (the right column).

Figure 6C. The seasonal variation of longitudinal averaged SO<sub>2</sub> emission from MEIC [g S/m<sup>2</sup>/year].

Revised Figure 11.

C10

Revised Figure 7. Error bars stand for one standard deviations of the observations.  
Revised Figure 9. Error bars stand for one standard deviations of the observations.

References: Bhawar, R. L., Lee, W.-S., and Pahu, I. P.R.C.: Aerosol types and radiative forcing estimates over East Asia, *Atmos. Environ.*, 141, 532-541, doi:10.1016/j.atmosenv.2016.07.028, 2016. Chen, D., Liu, Z., Fast, J., and Ban, J.: Simulations of sulfate-nitrate-ammonium (SNA) aerosols during the extreme haze events over northern China in October 2014. *Atmos. Chem. Phys.*, 16, 10707-10724, doi:10.5194/acp-16-10707-2016, 2016. Dong, X., Fu, J. S., Huang, K., Tong, D., and Zhuang, G.: Model development of dust emission and heterogeneous chemistry within the Community Multiscale Air Quality modeling system and its application over East Asia. *Atmos. Chem. Phys.*, 16, 8157-8180, doi:10.5194/acp-16-8157-2016, 2016. Geng, N., Wang, J., Xu, Y., Zhang, W., Chen, C., and Zhang, R.: PM<sub>2.5</sub> in an industrial district of Zhengzhou, China: chemical composition and source apportionment, *Partic-uology*, 11(1), 99-109, 2013. He, H., Wang, Y., Ma, Q., Ma, J., Chu, B., Ji, D., Tang, G., Liu, C. Zhang, H., and Hao, J.: Mineral dust and NO<sub>x</sub> promote the conversion of SO<sub>2</sub> to sulfate in heavy pollution days. *Sci. Rep.*, 4, 4172, doi:10.1038/srep04172, 2014. Huang, X., Song, Y., Zhao, C., Li, M., Zhu, T., Zhang, Q., and Zhang, X.: Pathways of sulfate enhancement by natural and anthropogenic mineral aerosols in China. *J. Geophys. Res.*, 119, 14165-14179, doi:10.1002/2014JD022301, 2014. Lu, Z., Zhang Q., and Streets D. G.: Sulfur dioxide and primary carbonaceous aerosol emissions in China and India, 1996–2010 *Atmos. Chem. Phys.*, 11, 9839–9864, doi:10.5194/acp-11-9839-2011, 2011. Li, Jiandong, Wei-Chyung Wang, Zhian Sun, Guoxiong Wu, Hong Liao, Yimin Liu, Decadal variation of East Asian radiative forcing due to anthropogenic aerosols during 1850–2100, and the role of atmospheric moisture, *Clim Res*, Vol. 61: 241–257, doi: 10.3354/cr01236, 2014. Paulot F, Fan S, Horowitz L W.: Contrasting seasonal responses of sulfate aerosols to declining SO<sub>2</sub> emissions in the Eastern US: implications for the efficacy of SO<sub>2</sub> emission controls, *Geophys. Res. Lett.*, 2016. Streets, D. G., Bond, T. C., Carmichael, G. R., Fernandes, S. D., Fu, Q., He, D., Klimont, Z., Nelson, S. M., Tsai, N. Y., Wang, M. Q., Woo, J.-H., and

C11

Yarber, K. F.: An inventory of gaseous and primary aerosol emissions in Asia in the year 2000, *J. Geophys. Res.*, 108, 8809, doi:10.1029/2002JD003093, 2003. Wang, Y., Zhang, Q., Jiang, J., Zhou, W.: Enhanced sulfate formation during China's severe winter haze episode in January 2013 missing from current models. *J. Geophys. Res.*, 119, 10,425-10,440, doi:10.1002/2013JD021426, 2014. Wang, Y. S., Yao, L., Wang, L., Liu, Z., et al.: Mechanism for the formation of the January 2013 heavy haze pollution episode over central and eastern China." *Science China-Earth Sciences*, 57(1): 14-25, 2014. Wang G, Zhang R, Gomez M E, et al. :Persistent sulfate formation from London Fog to Chinese haze., *Proceedings of the Nat. Acad. of Sci.*, 201616540, 2016. Westervelt, D. M., Horowitz, L.W., Naik. V., et al: Radiative forcing and climate response to projected 21st century aerosol decreases. *Atmos. Chem. and Phys.*, 15(22): 12681-12703, 2015. Zhang, R., Jing, J., Tao, J., Hsu, S.-C., Wang, G., Cao, J., Lee, C. S. L., Zhu, L., Chen, Z., Zhao, Y., and Shen, Z.: Chemical characterization and source apportionment of PM<sub>2.5</sub> in Beijing: seasonal perspective, *Atmos. Chem. Phys.*, 13(14), 7053-7074, 2013. Zhao, P. S., Dong, F., He, D., Zhao, X. J., Zhang, X. L., Zhang, W. Z., Yao, Q., and Liu, H. Y.: Characteristics of concentrations and chemical compositions for PM<sub>2.5</sub> in the region of Beijing, Tianjin, and Hebei, China, *Atmos. Chem. Phys.*, 13, 4631-4644, 2013. Zheng, B., Zhang, Q., Zhang, Y., He, K. and et al.: Heterogeneous chemistry: a mechanism missing in current models to explain secondary inorganic aerosol formation during the January 2013 haze episode in North China. *Atmos. Chem. Phys.*, 15, 2031-2049, doi:10.5194/acp-15-2031-2015, 2015.

Interactive comment on *Atmos. Chem. Phys. Discuss.*, doi:10.5194/acp-2016-802, 2016.

C12

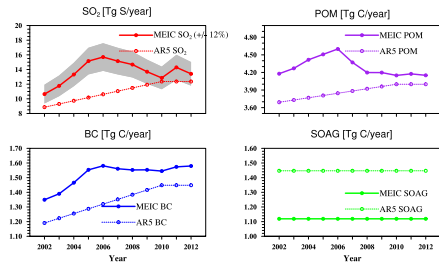


Fig. 1. Fig 1C

C13

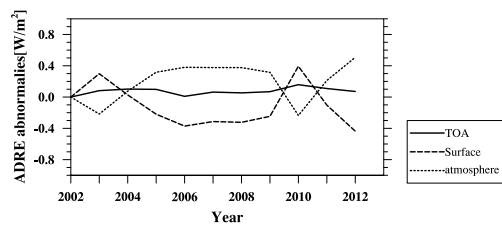


Fig. 2. Fig 2C

C14

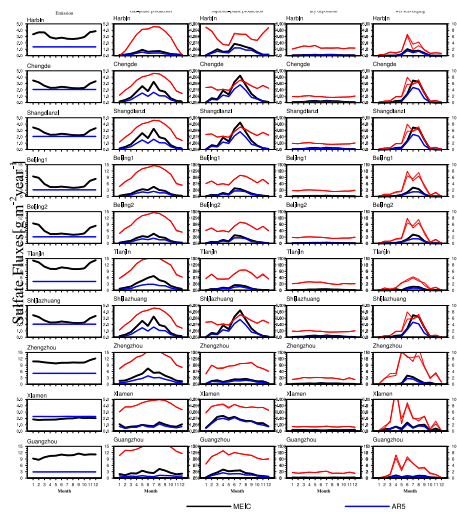


Fig. 3. Fig 3C

C15

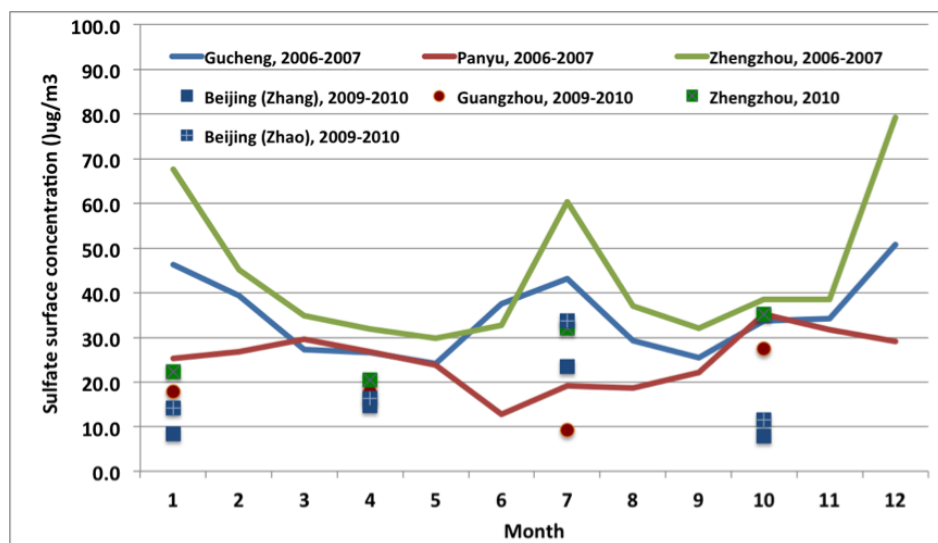


Fig. 4. Fig 4C

C16



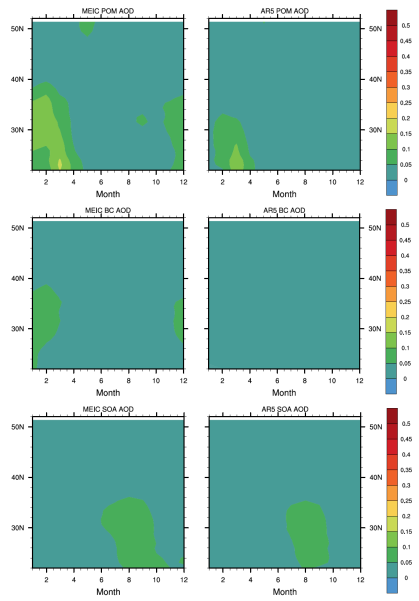


Fig. 5. Fig S1.

C17

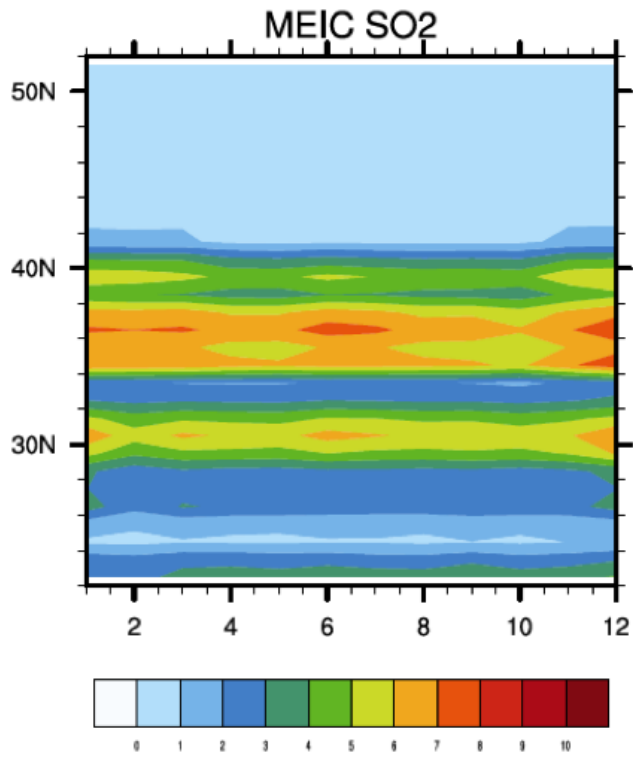


Fig. 6. Fig 6C

C18

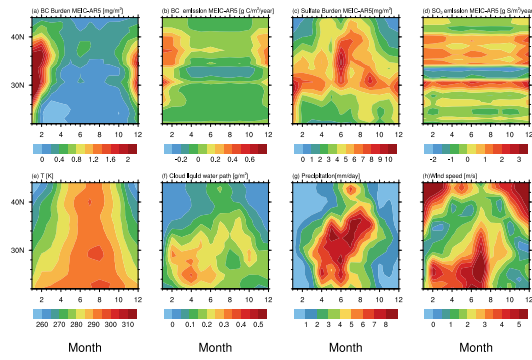


Fig. 7. Revised Fig 11

C19

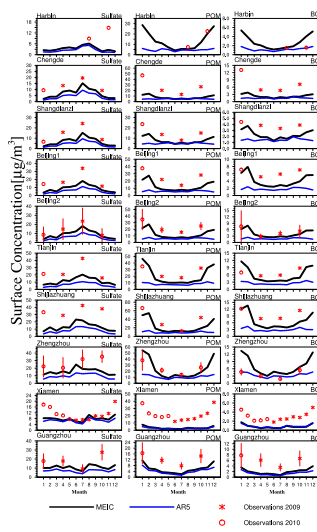


Fig. 8. Revised Fig 9

C20